

On Best Linear Unbiased Estimator Approach for Time-of-Arrival based Localization

Frankie K. W. Chan, H. C. So, Jun Zheng and Kenneth W. K. Lui

Department of Electronic Engineering, City University of Hong Kong
Tat Chee Avenue, Kowloon, Hong Kong

Email: k.w.chan@student.cityu.edu.hk, hcso@ee.cityu.edu.hk, junzheng@cityu.edu.hk
50469990@student.cityu.edu.hk

January 30, 2008

Keywords: *time-of-arrival, fast algorithm, position estimation, weighted least squares*

Abstract

A common technique for source localization is to utilize the time-of-arrival (TOA) measurements between the source and several spatially separated sensors. The TOA information defines a set of circular equations from which the source position can be calculated with the knowledge of the sensor positions. Apart from nonlinear optimization, least squares calibration (LSC) and linear least squares (LLS) are two computationally simple positioning alternatives which reorganize the circular equations into a unique and non-unique set of linear equations, respectively. As the LSC and LLS algorithms employ standard least squares (LS), an obvious improvement is to utilize weighted LS estimation. In this paper, it is proved that the best linear unbiased estimator (BLUE) version of the LLS algorithm will give identical estimation performance as long as the linear equations correspond to the independent set. The equivalence of the BLUE-LLS approach and the BLUE variant of the LSC method is analyzed. Simulation results are also included to show the comparative performance of the BLUE-LSC, BLUE-LLS, LSC, LLS and constrained weighted LSC methods with Cramér-Rao lower bound.

1 Introduction

Source localization using measurements from an array of spatially separated sensors has been an important problem in radar, sonar, global positioning system [1], mobile communications [2], multimedia [3] and wireless sensor networks [4]. One commonly used location-bearing parameter is the time-of-arrival (TOA) [2],[4], that is, the one-way signal propagation or round trip time between the source and sensor. For two-dimensional positioning, each noise-free TOA provides a circle centered at the sensor on which the source must lie. By using $M \geq 3$ sensors, the source location can be uniquely determined by the intersection of circles. In practice, the TOA measurements are noisy which implies multiple intersection points and thus they are usually converted into a set of circular equations, from which the source position is estimated with the knowledge of the signal propagation speed and sensor array geometry.

Commonly used techniques for solving the circular equations include linearization via Taylor-series expansion [5] and steepest descent method [6]. Although this direct approach can attain optimum estimation performance, it is computationally intensive and sufficiently precise initial estimates are required to obtain the global solution. On the other hand, an alternative approach which allows real-time computation and ensures global convergence is to reorganize the nonlinear equations into a set of linear equations by introducing an extra variable that is a function of the source position. It is noteworthy that this idea is first introduced in [7]-[8] for time-difference-of-arrival (TDOA) based localization. The linear equations can then be solved straightforwardly by using least squares and the corresponding estimator is referred to as the least squares calibration (LSC) method [9], or by eliminating the common variable via subtraction of each equation from all others, which is referred to as the linear least squares (LLS) estimator [10]-[11]. In this work, we will focus on relationship development between the the best linear unbiased estimator (BLUE) [12] versions of the LSC and LLS algorithms. Our contributions do not lie on new positioning algorithm development as the BLUE technique for localization applications has already been proposed in the literature [13]. Our major findings include (i) All BLUE realizations of the LLS algorithm have identical estimation performance as long as the $(M - 1)$ linear equations correspond to the independent set [10]; (ii) The covariance matrices of the position estimates in the BLUE-LLS scheme with the independent set and the BLUE version of the LSC algorithm are identical. By comparing with Cramér-Rao lower bound (CRLB) for TOA-based localization [14], it is then shown that they are suboptimal estimators, and this result is different from the iterative BLUE estimator of [13] which gives maximum likelihood estimation performance; and (iii) Among the BLUE-LLS and BLUE-LSC algorithms, the latter is preferable as it involves lower computational complexity. Note that the research results can also be applied to source localization systems with received signal strength [2] measurements as they employ the same trilateration concept where the propagation path losses from the source to the sensors are measured

to give their distances.

The organization of this paper is as follows. In Section 2, we first develop the weighted versions of the LSC and LLS methods based on BLUE. The equivalences between various forms of the BLUE-LLS solutions within the independent set and the BLUE-LSC estimate are then proved. Furthermore, their suboptimality and computational requirement will be discussed. Simulation results are included in Section 3 to evaluate the estimation performance of the BLUE-LSC and BLUE-LLS algorithms by comparing with the LSC, LLS and constrained weighted LSC [14] methods as well as verify our theoretical development. Finally, conclusions are drawn in Section 4.

2 Best Linear Unbiased Estimator based Positioning

In this Section, we first present the signal model for TOA-based localization. The BLUE-LSC and BLUE-LLS algorithms are then devised from the LSC and LLS formulations, respectively. Their relationship, estimation performance and computational complexity are also provided.

Let (x, y) and (x_i, y_i) , $i = 1, 2, \dots, M$, be the unknown source position and the known coordinates of the i th sensor, respectively. With known signal propagation speed, the range measurements between the source and sensors are straightforwardly determined from the corresponding TOA measurements, which are modelled as

$$r_i = d_i + n_i, \quad i = 1, 2, \dots, M \quad (1)$$

where $d_i = \sqrt{(x - x_i)^2 + (y - y_i)^2}$ is the noise-free range and n_i is the noise in r_i . For simplicity, we assume line-of-sight propagation between the source and all sensors such that each n_i is a zero-mean white process with known variance σ_i^2 [14].

2.1 BLUE-LSC Algorithm

BLUE [12] is a linear estimator which is unbiased and has minimum variance among all other linear estimators. In order to employ the BLUE technique, we need to restrict the parameters to be estimated linear in the data. It is suitable for practical implementation as only the mean and covariance of the data are required and complete knowledge of the probability density function is not necessary. The BLUE version of the LSC estimator is derived as follows.

Squaring both sides of (1), we have [9]:

$$x_i x + y_i y - 0.5R = \frac{1}{2} (x_i^2 + y_i^2 - r_i^2) + m_i, \quad i = 1, 2, \dots, M \quad (2)$$

where $m_i = n_i^2/2 + d_i n_i$ and $R = x^2 + y^2$ is the introduced variable to reorganize (1) into a set of linear equations in x , y and R . To facilitate the development, we express (2) in matrix form:

$$\mathbf{A}\boldsymbol{\theta} + \mathbf{p} = \mathbf{b} \quad (3)$$

where

$$\mathbf{A} = \begin{bmatrix} x_1 & y_1 & -0.5 \\ \vdots & \vdots & \vdots \\ x_M & y_M & -0.5 \end{bmatrix}$$

$$\boldsymbol{\theta} = \begin{bmatrix} x \\ y \\ R \end{bmatrix}$$

$$\mathbf{p} = \begin{bmatrix} -m_1 \\ \vdots \\ -m_M \end{bmatrix}$$

and

$$\mathbf{b} = \frac{1}{2} \begin{bmatrix} x_1^2 + y_1^2 - r_1^2 \\ \vdots \\ x_M^2 + y_M^2 - r_M^2 \end{bmatrix}$$

For sufficiently small noise conditions, $\mathbf{p} \approx [-d_1 n_1 \cdots -d_M n_M]^T$ and $E\{r_i^2\} \approx d_i^2$, $i = 1, 2, \dots, M$, where T denotes transpose operation and E is the expectation operator. Hence we have $E\{\mathbf{b}\} \approx \mathbf{A}\boldsymbol{\theta}$ which corresponds to the linear unbiased data model. Using the information that \mathbf{p} is approximately zero-mean and its covariance matrix, denoted by \mathbf{C}_p , is a diagonal matrix of the form:

$$\mathbf{C}_p \approx \begin{bmatrix} d_1^2 \sigma_1^2 & 0 & \cdots & 0 \\ 0 & d_2^2 \sigma_2^2 & \cdots & 0 \\ \vdots & \vdots & \ddots & \vdots \\ 0 & 0 & \cdots & d_M^2 \sigma_M^2 \end{bmatrix} \quad (4)$$

The BLUE for $\boldsymbol{\theta}$ based on (3), denoted by $\hat{\boldsymbol{\theta}}$, is then [12]:

$$\hat{\boldsymbol{\theta}} = (\mathbf{A}^T \mathbf{C}_p^{-1} \mathbf{A})^{-1} \mathbf{A}^T \mathbf{C}_p^{-1} \mathbf{b} \quad (5)$$

where $^{-1}$ represents matrix inverse. Note that the LSC estimate is given by (5) with the substitution of $\mathbf{C}_p = \mathbf{I}_M$ where \mathbf{I}_M is the $M \times M$ identity matrix, without utilizing the mean and covariance of the data. Since $\{d_i\}$ are unknown, they will be substituted by $\{r_i\}$ in practice. The covariance matrix for $\hat{\boldsymbol{\theta}}$, denoted by \mathbf{C}_θ , is [12]:

$$\mathbf{C}_\theta \approx (\mathbf{A}^T \mathbf{C}_p^{-1} \mathbf{A})^{-1} \quad (6)$$

where the variances for the estimates of x and y are given by the (1,1) and (2,2) entries of \mathbf{C}_θ , respectively. It is worthy to mention that the same weighting matrix of \mathbf{C}_p^{-1} has been proposed in [14], which can be considered as a constrained weighted least squares calibration (CWLSC) algorithm with utilizing the constraint of $x^2 + y^2 = R$. We expect that the BLUE-LSC algorithm is inferior to the CWLSC scheme as the parameter relationship in θ is not exploited.

2.2 BLUE-LLS Algorithm

On the other hand, subtracting the first equation of (2) from the remaining equations, R can be eliminated and we get $(M - 1)$ equations:

$$(x_i - x_1)x + (y_i - y_1)y = \frac{1}{2} (x_i^2 + y_i^2 - x_1^2 - y_1^2 - r_i^2 + r_1^2) + m_i - m_1, \quad i = 2, 3, \dots, M \quad (7)$$

Expressing (7) in matrix form yields

$$\mathbf{G}\phi + \mathbf{q} = \mathbf{h} \quad (8)$$

where

$$\mathbf{G} = \begin{bmatrix} x_2 - x_1 & y_2 - y_1 \\ \vdots & \vdots \\ x_M - x_1 & y_M - y_1 \end{bmatrix}$$

$$\phi = \begin{bmatrix} x \\ y \end{bmatrix}$$

$$\mathbf{q} = \begin{bmatrix} m_1 - m_2 \\ \vdots \\ m_1 - m_M \end{bmatrix}$$

and

$$\mathbf{h} = \frac{1}{2} \begin{bmatrix} x_2^2 + y_2^2 - x_1^2 - y_1^2 - r_2^2 + r_1^2 \\ \vdots \\ x_M^2 + y_M^2 - x_1^2 - y_1^2 - r_M^2 + r_1^2 \end{bmatrix}$$

Following the development of the BLUE-LSC algorithm, the BLUE-LLS estimate for ϕ based on (8), denoted by $\hat{\phi}$, is:

$$\hat{\phi} = (\mathbf{G}^T \mathbf{C}_q^{-1} \mathbf{G})^{-1} \mathbf{G}^T \mathbf{C}_q^{-1} \mathbf{h} \quad (9)$$

where \mathbf{C}_q is the covariance matrix for \mathbf{q} which has the form of

$$\mathbf{C}_q \approx \begin{bmatrix} d_1^2 \sigma_1^2 + d_2^2 \sigma_2^2 & d_1^2 \sigma_1^2 & \cdots & d_1^2 \sigma_1^2 \\ d_1^2 \sigma_1^2 & d_1^2 \sigma_1^2 + d_3^2 \sigma_3^2 & \cdots & d_1^2 \sigma_1^2 \\ \vdots & \vdots & \ddots & \vdots \\ d_1^2 \sigma_1^2 & d_1^2 \sigma_1^2 & \cdots & d_1^2 \sigma_1^2 + d_M^2 \sigma_M^2 \end{bmatrix} \quad (10)$$

With the use of matrix inversion lemma, its inverse can be computed as:

$$\mathbf{C}_q^{-1} \approx \text{diag} \left(\frac{1}{d_2^2 \sigma_2^2}, \frac{1}{d_3^2 \sigma_3^2}, \dots, \frac{1}{d_M^2 \sigma_M^2} \right) - \frac{1}{\sum_{i=1}^M \frac{1}{d_i^2 \sigma_i^2}} \begin{bmatrix} \frac{1}{d_2^4 \sigma_2^4} & \frac{1}{d_2^2 d_3^2 \sigma_2^2 \sigma_3^2} & \cdots & \frac{1}{d_2^2 d_M^2 \sigma_2^2 \sigma_M^2} \\ \frac{1}{d_3^2 d_2^2 \sigma_3^2 \sigma_2^2} & \frac{1}{d_3^4 \sigma_3^4} & \cdots & \frac{1}{d_3^2 d_M^2 \sigma_3^2 \sigma_M^2} \\ \vdots & \vdots & \ddots & \vdots \\ \frac{1}{d_M^2 d_1^2 \sigma_M^2 \sigma_1^2} & \frac{1}{d_M^2 d_3^2 \sigma_M^2 \sigma_3^2} & \cdots & \frac{1}{d_M^4 \sigma_M^4} \end{bmatrix} \quad (11)$$

Note that the LLS estimate is given by (9) with the substitution of $\mathbf{C}_q = \mathbf{I}_{M-1}$, without utilizing the mean and covariance of the data. The estimator of (9) has minimum variance according to the data model of (8). It is worthy to note that although the dependent variable of R is eliminated in the LLS approach, estimation performance degradation occurs in the conversion of (2) to (7) or (8). This is analogous to TOA-based and TDOA-based positioning where the former estimation performance bound is lower than that of the latter if the TDOAs are obtained from subtraction between the TOAs [15]-[16]. The covariance matrix for $\hat{\phi}$, denoted by \mathbf{C}_ϕ , is:

$$\mathbf{C}_\phi \approx (\mathbf{G}^T \mathbf{C}_q^{-1} \mathbf{G})^{-1} \quad (12)$$

Although there are at most $M(M-1)$ LLS equations can be generated from (2), only $(M-1)$ are independent [10]. In fact, (7) is an example of the independent set of equations. Although we can use up to $M(M-1)$ dependent equations in the standard LLS algorithm, this is not possible for the BLUE realization because the corresponding noise covariance matrix will be singular. In the following, we will prove that as long as the $(M-1)$ equations belong to the independent set, the BLUE-LLS estimator performance will agree with the covariance matrices given by (6) and (12). Their suboptimality is then illustrated by contrasting with the CRLB.

First, we define two sets:

$$\Xi = \{\mathbf{e}_{M,i} - \mathbf{e}_{M,j} : i, j = 1, 2, \dots, M, i \neq j \text{ and } \mathbf{e}_{m,n} \text{ is the } n\text{th column of } \mathbf{I}_m\} \quad (13)$$

and

$$\Theta = \left\{ \boldsymbol{\xi} \in \mathbb{R}^{(M-1) \times M} : \boldsymbol{\xi}^T \mathbf{e}_{M-1,k} \in \Xi, k = 1, 2, \dots, M \text{ and } \text{rank}(\boldsymbol{\xi}) = M-1 \right\} \quad (14)$$

where Θ corresponds to all independent sets of the LLS equations. In doing so, we can generalize (8) as:

$$\mathbf{KAL}\phi + \mathbf{Kp} = \mathbf{Kb} \quad (15)$$

for any $\mathbf{K} \in \Theta$ where $\mathbf{L}^T = [\mathbf{I}_2 \ \mathbf{0}_{2 \times 1}]$ with $\mathbf{0}_{M \times N}$ denotes the $M \times N$ zero matrix. As a result, the general BLUE-LLS estimate and its covariance matrix are then:

$$\hat{\phi} = \left(\mathbf{L}^T \mathbf{A}^T \mathbf{K}^T (\mathbf{K} \mathbf{C}_p \mathbf{K}^T)^{-1} \mathbf{K} \mathbf{A} \mathbf{L} \right)^{-1} \mathbf{L}^T \mathbf{A}^T \mathbf{K}^T (\mathbf{K} \mathbf{C}_p \mathbf{K}^T)^{-1} \mathbf{K} \mathbf{b} \quad (16)$$

and

$$\mathbf{C}_\phi \approx \left(\mathbf{L}^T \mathbf{A}^T \mathbf{K}^T (\mathbf{K} \mathbf{C}_p \mathbf{K}^T)^{-1} \mathbf{K} \mathbf{A} \mathbf{L} \right)^{-1} \quad (17)$$

As an illustration, substituting $\mathbf{K} = [-\mathbf{1}_{M-1} \ \mathbf{I}_{M-1}]$ in (16) and (17), where $\mathbf{1}_{M-1}$ is a column vector of length $M - 1$ with all elements equal 1, yield (9) and (12).

2.3 Relationship and Performance

Using the property of $\mathbf{K} \mathbf{1}_M = \mathbf{0}_{(M-1) \times 1}$, we construct an idempotent matrix $\mathbf{B} \in \mathbb{R}^{M \times M}$ which has the form of:

$$\mathbf{B} = \frac{\mathbf{C}_p^{-\frac{1}{2}} \mathbf{1}_M \mathbf{1}_M^T \mathbf{C}_p^{-\frac{1}{2}}}{\text{tr}(\mathbf{C}_p^{-1})} + \mathbf{C}_p^{\frac{1}{2}} \mathbf{K}^T (\mathbf{K} \mathbf{C}_p \mathbf{K}^T)^{-1} \mathbf{K} \mathbf{C}_p^{\frac{1}{2}} \quad (18)$$

where tr is the trace operator. Since $\text{rank}(\mathbf{B}) = \text{tr}(\mathbf{B})$ and the traces of the first and second terms in (18) can be computed as 1 and $(M - 1)$, respectively, we get $\text{rank}(\mathbf{B}) = M$. Employing the full rank property of \mathbf{B} as well as idempotent property of $\mathbf{B}(\mathbf{I}_M - \mathbf{B}) = \mathbf{0}_{M \times M}$ yield

$$\mathbf{B} = \mathbf{I}_M \quad (19)$$

With the use of (19), we pre-multiply and post-multiply both sides of (18) by $\mathbf{C}_p^{-\frac{1}{2}}$ to obtain

$$\mathbf{K}^T (\mathbf{K} \mathbf{C}_p \mathbf{K}^T)^{-1} \mathbf{K} = \mathbf{C}_p^{-1} - \frac{\mathbf{C}_p^{-1} \mathbf{1}_M \mathbf{1}_M^T \mathbf{C}_p^{-1}}{\text{tr}(\mathbf{C}_p^{-1})} \quad (20)$$

Hence the value of $\mathbf{K}^T (\mathbf{K} \mathbf{C}_p \mathbf{K}^T)^{-1} \mathbf{K}$ will be identical for all $\mathbf{K} \in \Theta$, which implies that all variants of the BLUE-LLS algorithms have the same covariance matrix of (12).

Furthermore, the covariance matrix for the estimates of x and y in the BLUE-LSC algorithm can be expressed as $\mathbf{L}^T (\mathbf{A}^T \mathbf{C}_p^{-1} \mathbf{A})^{-1} \mathbf{L}$, which corresponds to the upper left 2×2 sub-matrix of $(\mathbf{A}^T \mathbf{C}_p^{-1} \mathbf{A})^{-1}$:

$$(\mathbf{A}^T \mathbf{C}_p^{-1} \mathbf{A})^{-1} = \begin{bmatrix} \mathbf{L}^T \mathbf{A}^T \mathbf{C}_p^{-1} \mathbf{A} \mathbf{L} & -0.5 \mathbf{L}^T \mathbf{A}^T \mathbf{C}_p^{-1} \mathbf{1}_M \\ -0.5 \mathbf{1}_M^T \mathbf{C}_p^{-1} \mathbf{A} \mathbf{L} & 0.25 \mathbf{1}_M^T \mathbf{C}_p^{-1} \mathbf{1}_M \end{bmatrix}^{-1} \quad (21)$$

With the use of the partitioned inversion formula, $\mathbf{L}^T (\mathbf{A}^T \mathbf{C}_p^{-1} \mathbf{A})^{-1} \mathbf{L}$ is computed as

$$\mathbf{L}^T (\mathbf{A}^T \mathbf{C}_p^{-1} \mathbf{A})^{-1} \mathbf{L} = \left(\mathbf{L}^T \mathbf{A}^T \left(\mathbf{C}_p^{-1} - \frac{\mathbf{C}_p^{-1} \mathbf{1}_M \mathbf{1}_M^T \mathbf{C}_p^{-1}}{\text{tr}(\mathbf{C}_p^{-1})} \right) \mathbf{A} \mathbf{L} \right)^{-1} \quad (22)$$

From (17), (20) and (22), we easily see that the estimation performance of the BLUE-LLS and BLUE-LSC algorithms is essentially identical.

Assuming that $\{n_i\}$ are Gaussian distributed, comparison of (12) and the CRLB for positioning is made as follows. Denote the corresponding Fisher information matrix by \mathbf{D}^{-1} , which has the form of [14]

$$\mathbf{D}^{-1} = \mathbf{F}^T \mathbf{C}_p^{-1} \mathbf{F} \quad (23)$$

where

$$\mathbf{F} = \begin{bmatrix} x - x_1 & y - y_1 \\ x - x_2 & y - y_2 \\ \vdots & \vdots \\ x - x_M & y - y_M \end{bmatrix}$$

Exploiting $\mathbf{G} = -\mathbf{K}\mathbf{F}$ and $\mathbf{C}_q = \mathbf{K}\mathbf{C}_p\mathbf{K}^T$ and with the use of (12) and (20), the inverse of \mathbf{C}_ϕ can be expressed as

$$\mathbf{C}_\phi^{-1} = \mathbf{F}^T \left(\mathbf{C}_p^{-1} - \frac{\mathbf{C}_p^{-1} \mathbf{1}_M \mathbf{1}_M^T \mathbf{C}_p^{-1}}{\text{tr}(\mathbf{C}_p^{-1})} \right) \mathbf{F} \quad (24)$$

From (23) and (24), we have

$$\mathbf{D}^{-1} - \mathbf{C}_\phi^{-1} = \mathbf{F}^T \frac{\mathbf{C}_p^{-1} \mathbf{1}_M \mathbf{1}_M^T \mathbf{C}_p^{-1}}{\text{tr}(\mathbf{C}_p^{-1})} \mathbf{F} \quad (25)$$

which is positive semidefinite. This implies that $\mathbf{C}_\phi - \mathbf{D}$ is also positive semidefinite, and thus the variances of the BLUE-LLS estimates of x and y are greater than or equal to their corresponding performance limits.

2.4 Complexity Analysis

Finally, the computational complexity of the linear equation based algorithms is investigated. The numbers of multiplications and additions, denoted by \mathcal{M} and \mathcal{A} , respectively, required in the BLUE-LSC, LSC, BLUE-LLS and LLS algorithms are provided in Table I which clearly shows the calculation breakdown. Note that the Gaussian elimination is employed for performing the matrix inverse operation. In particular, we have assumed the covariance matrix of (10) which has a closed-form inverse in the BLUE-LLS method. Excluding the computationally extensive task of solving the Lagrange multiplier corresponding to the constraint of $x^2 + y^2 = R$, the CWLSC method needs $(16M + 24)$ multiplications and $(10M + 7)$ additions. Although the BLUE-LSC and BLUE-LLS methods are identical, we see that the former is preferable because it is more computationally attractive. Furthermore, the computational requirement of the BLUE-LSC estimator is comparable with those of the LSC and LLS schemes and is significantly less than that of the CWLSC method.

	BLUE-LSC	LSC	BLUE-LLS	LLS
\mathbf{G}, \mathbf{A}	0	0	$2M \mathcal{A}$	$2M \mathcal{A}$
$\mathbf{C}_p, \mathbf{C}_q$	$3M \mathcal{M}$	0	$3M \mathcal{M}$ $M \mathcal{A}$	0
$\mathbf{C}_p^{-1}, \mathbf{C}_q^{-1}$	$M \mathcal{M}$	0	$0.5M^2 + 1.5M \mathcal{M}$ $M - 1 \mathcal{A}$	0
$\mathbf{A}^T \mathbf{C}_p^{-1},$ $\mathbf{G}^T \mathbf{C}_q^{-1}$	$2M + 1 \mathcal{M}$	0	$2M^2 - 4M + 2 \mathcal{M}$ $2M^2 - 6M + 4 \mathcal{A}$	0
$\mathbf{A}^T \mathbf{C}_p^{-1} \mathbf{A},$ $\mathbf{G}^T \mathbf{C}_q^{-1} \mathbf{G}$	$3M + 4 \mathcal{M}$ $5M - 5 \mathcal{A}$	$3M + 4 \mathcal{M}$ $5M - 5 \mathcal{A}$	$3M - 3 \mathcal{M}$ $3M - 6 \mathcal{A}$	$3M - 3 \mathcal{M}$ $3M - 6 \mathcal{A}$
\mathbf{b}, \mathbf{h}	$4M \mathcal{M}$ $2M \mathcal{A}$	$4M \mathcal{M}$ $2M \mathcal{A}$	$4M \mathcal{M}$ $3M - 1 \mathcal{A}$	$4M \mathcal{M}$ $3M - 1 \mathcal{A}$
$\mathbf{A}^T \mathbf{C}_p^{-1} \mathbf{b},$ $\mathbf{G}^T \mathbf{C}_q^{-1} \mathbf{h}$	$3M \mathcal{M}$ $3M - 3 \mathcal{A}$	$3M \mathcal{M}$ $3M - 3 \mathcal{A}$	$2M - 2 \mathcal{M}$ $2M - 4 \mathcal{A}$	$2M - 2 \mathcal{M}$ $2M - 4 \mathcal{A}$
Gaussian Elimination	$17 \mathcal{M}$ $14 \mathcal{A}$	$17 \mathcal{M}$ $14 \mathcal{A}$	$6 \mathcal{M}$ $4 \mathcal{A}$	$6 \mathcal{M}$ $4 \mathcal{A}$
Total	$16M + 22 \mathcal{M}$ $10M + 6 \mathcal{A}$	$10M + 21 \mathcal{M}$ $10M + 6 \mathcal{A}$	$2.5M^2 + 9.5M + 3 \mathcal{M}$ $2M^2 + 6M - 4 \mathcal{A}$	$9M + 1 \mathcal{M}$ $10M - 7 \mathcal{A}$

Table 1: Breakdown of computational complexity

3 Numerical Examples

Computer simulations have been conducted to evaluate the performance of the BLUE-LSC and BLUE-LLS algorithms by comparing with the LLS, LSC and CWLSC [14] algorithms as well as CRLB. The BLUE-LLS method is implemented using the form of (9). The range errors $\{n_i\}$ are zero-mean white Gaussian processes. All results were averages of 1000 independent runs.

We first consider a mobile positioning scenario with 4 sensors of known coordinates (3000, 3000)m, (3000, -3000)m, (-3000, 3000)m and (-3000, -3000)m. Figure 1 plots the mean square position errors (MSPEs) of the positioning methods versus average noise power when the source is at $(x, y) = (1000, 2000)$ m. That is, the source is located inside the square bounded by the sensor coordinates. The MSPE is defined as $E\{(x - \hat{x})^2 + (y - \hat{y})^2\}$ where \hat{x} and \hat{y} denote the estimates of x and y , respectively, and the average noise power is given by $\sigma^2 = \frac{1}{M} \sum_{i=1}^M \sigma_i^2$, where σ_i^2 is chosen such that all $\{\sigma_i^2/d_i^2\}$ are kept identical. It is seen that the CWLSC scheme has the best estimation performance as its MSPE attains the CRLB when the average noise power is less than 70 dBm² where m is referenced to one meter or $\sigma = 10^{3.5}$ m. That is, the average noise power has a value of $10 \log_{10} \sigma^2$ in terms of dBm². Note that for larger noise conditions, the CWLSC method becomes a biased estimator as its MSPE is smaller than the CRLB. While the BLUE-LSC and BLUE-LLS algorithms are superior to the LLS and LSC methods for the whole noise range and their MSPEs are close to the CRLB when the average noise power is less than 80 dBm², which indicates the BLUE approach has a better threshold performance than that of CWLSC scheme. We also observe that the estimation performance of the LLS and LSC methods is different although their BLUE versions are identical. Moreover, the theoretical development of (6) or (12) is validated for sufficiently small noise powers, and the equivalence of the BLUE-LSC and BLUE-LLS algorithms is demonstrated. It is noteworthy that the average noise power range is reasonable for practical mobile location applications [17].

The above test is repeated for $(x, y) = (7000, 8000)$ m where the source is located outside the square. We see that the CWLSC algorithm attains the CRLB when the average noise power is less than 75 dBm². Although the BLUE approach is inferior to the CWLSC method, it has better threshold performance and still outperforms the standard LLS and LSC schemes. The theoretical development of (6) or (11) is again confirmed for sufficiently small noise conditions and the suboptimality as well as equivalence of the BLUE-LSC and BLUE-LLS methods are demonstrated.

Figure 3 plots the MSPEs of all the algorithms when the source position is randomly chosen in an area bounded by $(-6000\sqrt{2}, -6000\sqrt{2})$ m, $(-6000\sqrt{2}, 6000\sqrt{2})$ m, $(6000\sqrt{2}, -6000\sqrt{2})$ m and $(6000\sqrt{2}, 6000\sqrt{2})$ m for each trial. This means that approximately half of the mobile positions would be inside the region bounded by the sensor coordinates, and the remaining would be outside this region. As a result, the estimation performance of the methods differs at each trial because the positioning accuracy varies with the relative geometry between the source and sensors. Nevertheless, the

observations are similar to those in Figure 2.

Figure 4 shows the MSPEs of the algorithms versus number of receivers when the average noise power is kept at 40 dBm² with $(x, y) = (1000, 2000)$ m. We start with 3 sensors with known positions at $(0, 0)$ m, $(0, 3000\sqrt{3})$ m and $(3000\sqrt{3}, 0)$ m, and the sensors with coordinates $(-3000\sqrt{3}, 3000)$ m, $(-3000\sqrt{3}, -3000)$ m, $(0, -6000)$ m and $(3000\sqrt{3}, -3000)$ m are then added successively. Notice that variations in the sensor number also produces geometry changes and subsequently the positioning accuracy varies as well. In Figure 4, it is seen that the estimation accuracy of the CWLSC and BLUE methods increases with the number of receiving sensors while that of the LSC and LLS algorithm is loosely dependent on the sensor number. That is, the performance gain of employing the BLUE approach over the standard one is higher for a larger number of sensors. Again, (6) agrees well with the simulation results and the suboptimality as well as equivalence of the BLUE-LSC and BLUE-LLS methods are demonstrated.

4 Conclusion

Best linear unbiased estimator (BLUE) versions of the least squares calibration (LSC) and linear least squares (LLS) time-of-arrival based positioning algorithms have been examined. It is proved that various realizations of the BLUE-LLS approach are indifferent as long as the equations which correspond to the independent set are employed, and their estimation performance is identical to that of the BLUE-LSC algorithm. In spite of the suboptimality of the BLUE approach, its estimation accuracy can be close to Cramér-Rao lower bound particularly when the source is located inside the region bounded by sensor coordinates. Furthermore, the computational requirement of the BLUE-LSC algorithm is similar to that of the standard LSC and LLS methods and is significantly less than that of the constrained weighted LSC estimator which provides optimal positioning accuracy for sufficiently small noise conditions.

Acknowledgement

The authors would like to thank the anonymous reviewers for their careful reading and constructive comments, which improved the clarity of this paper. The work described in this paper was supported by a grant from the Research Grants Council of the Hong Kong Special Administrative Region, China (Project No. CityU 119606).

References

- [1] J.B. Tsui, *Fundamentals Of Global Positioning System Receivers*, New York, Chichester: John Wiley & Sons, 2000

- [2] J.J. Caffery, Jr., *Wireless Location in CDMA Cellular Radio Systems*, Boston: Kluwer Academic, 2000
- [3] S.L. Gay and J. Benesty, Eds., *Acoustic Signal Processing for Telecommunication*, Boston, London: Kluwer Academic, 2000
- [4] N. Patwari, J.N. Ash, S. Kyperountas, A.O. Hero, III, R.L. Moses and N.S. Correal, "Locating the nodes: cooperative localization in wireless sensor networks," *IEEE Signal Processing Magazine*, pp.54-69, July 2005
- [5] M.A. Spirito, "On the accuracy of cellular mobile station location estimation," *IEEE Trans. Veh. Technol.*, vol.50, pp.674-685, May 2001
- [6] J.J. Caffery, Jr. and G.L. Stuber, "Subscriber location in CDMA cellular networks," *IEEE Trans. Veh. Technol.*, vol.47 pp.406-416, May 1998
- [7] J.O. Smith and J.S. Abel, "Closed-form least-squares source location estimation from range-difference measurements," *IEEE Trans. Acoust., Speech, Signal Processing*, vol.35, pp.1661-1669, Dec. 1987
- [8] B. Friedlander, "A passive localization algorithm and its accuracy analysis," *IEEE J. Ocean. Eng.*, vol.12, pp.234-245, Jan. 1987
- [9] J.C. Chen, R.E. Hudson and K. Yao, "Maximum-likelihood source localization and unknown sensor location estimation for wideband signals in the near field," *IEEE Trans. Signal Processing*, vol.50, no.8, pp.1843-1854, Aug. 2002
- [10] A.J. Fenwick, "Algorithms for position fixing using pulse arrival times," *IEE Proc. - Radar, Sonar Navig.*, vol.146, no.4 pp.208-212, Aug. 1999
- [11] J.J. Caffery, Jr., "A new approach to the geometry of TOA location," *Proc. IEEE VTC 2000-Fall*, vol.4, pp.1943-1949, Sept. 2000
- [12] S.M. Kay, *Fundamentals of Statistical Signal Processing: Estimation Theory*, Englewood Cliffs, NJ: Prentice-Hall, 1993
- [13] S.D. Coutts, "3-D emitter localization using inhomogeneous bistatic scattering," *Proc. Int. Conf. Acoustics, Speech, and Signal Processing*, vol.3, pp.1509-1512, March 1999, Phoenix, USA
- [14] K.W. Cheung, H.C. So, W.-K. Ma and Y.T. Chan, "Least squares algorithms for time-of-arrival based mobile location," *IEEE Trans. on Signal Processing*, vol.52, no.4, pp.1121-1128, April 2004
- [15] M. McGuire and K.N. Plataniotis, "A comparison of radiolocation for mobile terminals by distance measurements", *Proc. Int. Conf. Wireless Communications*, pp.1356-1359, 2000

- [16] A. Urruela, J. Sala and J. Riba, "Average performance analysis of circular and hyperbolic geolocation," *IEEE Trans. Veh. Technol.*, vol.55, no.1, pp.52-66, Jan. 2006
- [17] C. Andersson, *GPRS and 3G Wireless Applications: Professional Developer's Guide*, New York: Wiley, pp.260, 2001

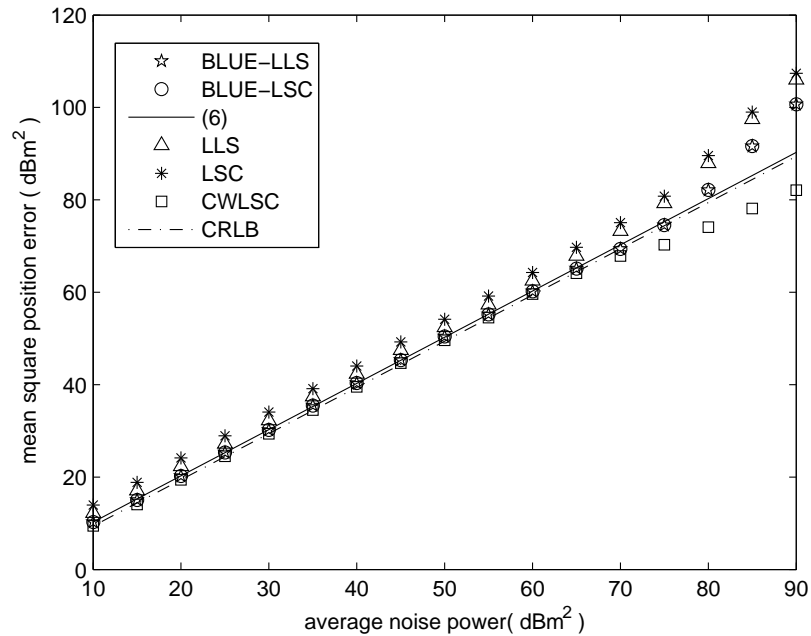


Figure 1: Mean square position errors at $(x, y) = (1000, 2000)$ m

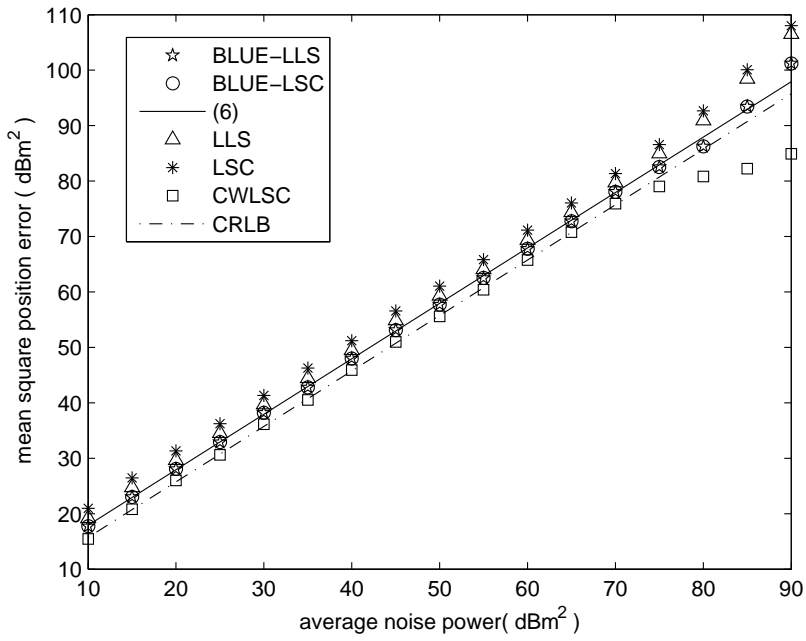


Figure 2: Mean square position errors at $(x, y) = (7000, 8000)m$

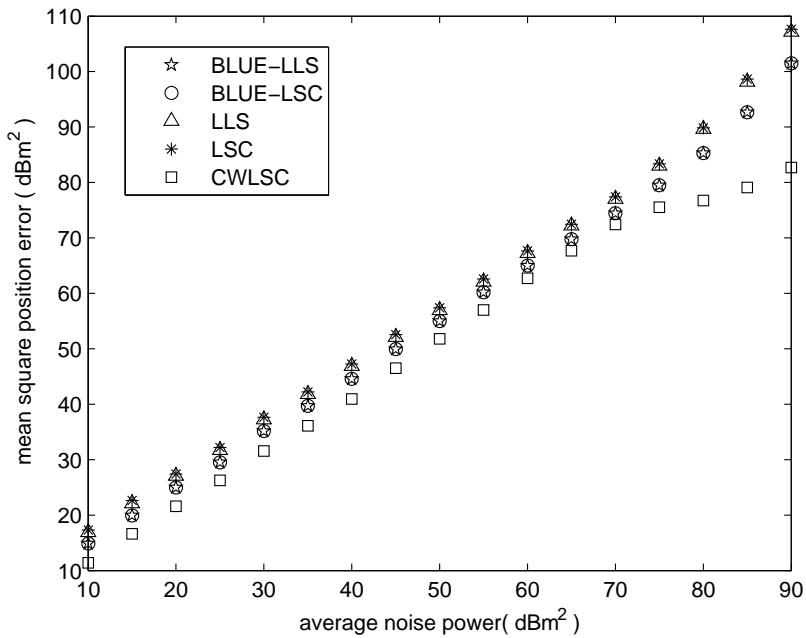


Figure 3: Mean square position errors with random source position

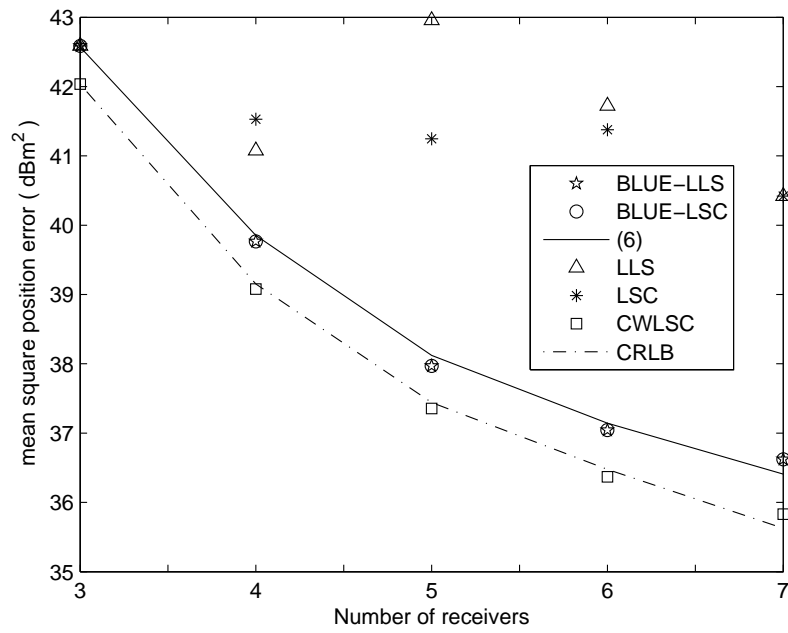


Figure 4: Mean square position errors versus number of receivers at $(x, y) = (1000, 2000)m$